Organic & Biomolecular Chemistry

RSC Publishing

PAPER

View Article Online
View Journal | View Issue

Cite this: *Org. Biomol. Chem.*, 2013, **11**, 5836

Solution and thermal behaviour of novel dicationic imidazolium ionic liquids†

Francesca D'Anna,*[a] H. Q. Nimal Gunaratne,[b] Giuseppe Lazzara,[c] Renato Noto,*[a] Carla Rizzo[a] and Kenneth R. Seddon[b]

Received 22nd April 2013,
Accepted 4th July 2013

DOI: 10.1039/c3ob40807h

www.rsc.org/obc

A new class of functionalised dicationic ionic liquids, containing a central cationic unit capped by a basic functionality (imidazole), has been synthesised. These salts have been characterised in isotropic solution using proton and 2D-NMR spectroscopy, and their thermal stability has been studied by DSC and TGA. All these novel salts contain the 1-(1-imidazolylmethyl)-3,5-di{1-(3′-octylimidazolylmethyl)}-benzene cation as a defining structural motif. Salts of both singly and doubly charged anions were prepared and, in particular, the selected monoanions (Br^-, $[BF_4]^-$, or $[NTf_2]^-$) differ in size, shape and hydrogen-bonding ability, whereas the dianions differ in the nature of the spacer, such as 1,4-benzenedicarboxylate, 2,6-naphthalenedicarboxylate, 1,5- and 2,6-naphthalenedisulfonate, 1,4-butanedicarboxylate, and 1,6-hexanedicarboxylate. These ionic liquids exhibit the presence of different conformers in solution, whose distribution is affected by the nature of the anion. The nature of the anion also affects their thermal stability.

Introduction

Efficiency, thermal stability and eco-sustainability are a trio of terms that have attracted the interest of the scientific community and have favoured the growth of ionic liquid research. Currently, thousands of ionic liquids are known of which the vast majority consists of monopositive cations.[1,2] Room temperature ionic liquids with dipositive cations are rare, hence their physical behaviour is not well understood.[3–9] Tripositive cations are even scarcer.[10–12] The interest in dicationic ionic liquids is largely due to their high thermal stability, higher than that normally characterising the corresponding monocationic ionic liquids. This has recently allowed their use as media when high temperatures are required.[13–16] In addition, their added stability has allowed them to be used for coating columns for use as stationary phases for capillary gas chromatography, showing both good coating properties and chromatographic separation abilities.[17] Moreover, the use of dicationic ionic liquids enables greater flexibility in tuning their physicochemical properties. In particular, the possibility of producing unsymmetrical dicationic or dianionic moieties creates a new opportunity to control ionic liquids properties. Indeed, both the nature of the dicationic head groups and the core structure may significantly affect the three-dimensional supramolecular structure.[18–21]

In terms of designing ionic liquids for specific applications, these dicationic ionic liquids open up the possibility of combining a resistance to high temperature with catalytic activity. In order to pursue this goal, the catalytic functionality could be situated on the anion, on the cationic head group, or alternatively on the spacer (for example, in the present case a benzene core), yielding multi-functionalised ionic liquids. To date, only a few dicationic functionalised ionic liquids have been reported in the literature, and in these cases the catalytic ability is due to specific properties of the anion,[22] or to the presence of an acid functionality on the cationic head.[23] In some other cases, the reported catalytic ability is a result of the formation of an organometallic complex.[24,25]

Here, we describe the structure–property relationships and thermal behaviour of a series of multi-positive imidazolium ionic liquids paired with multi-negative anions with respect to properties and applications.[26–30] In particular, we thought it could be interesting to study new dicationic ionic liquids functionalised with a basic moiety.[31] In order to pursue this goal, we chose 1,3,5-tris(bromomethyl)benzene as the key synthetic precursor and prepared nine functionalised dicationic salts bearing the 1-octylimidazolium ion as the cationic head group.

[a]*Dipartimento STEBICEF, Università degli Studi di Palermo, Viale delle Scienze-Parco d'Orleans II, 90128 Palermo, Italy. E-mail: francesca.danna@unipa.it, renato.noto@unipa.it; Fax: +39091596825; Tel: +3909123897535*
[b]*QUILL Research Centre, School of Chemistry and Chemical Engineering, The Queen's University of Belfast, Belfast BT9 5AG, Northern Ireland, UK. E-mail: quill@qub.ac.uk*
[c]*Dipartimento di Fisica e Chimica, Università degli Studi di Palermo, Viale delle Scienze-Parco d'Orleans II, 90128 Palermo, Italy*

†Electronic supplementary information (ESI) available: ^{1}H NMR and 2D NMR spectra, DSC and TGA traces and plot of correlation between $\Delta\delta$ (ppm) and T (K). See DOI: 10.1039/c3ob40807h

The third position of substitution on the central core was taken up by a neutral imidazole unit. This class of ionic liquids was hence characterised by the presence of the 1-(1-imidazolylmethyl)-3,5-di{1-(3′-octylimidazolylmethyl)}benzene cation $([2C_8bti]^{2+}$, where bti indicates a benzene-tris-imidazole unit bearing two octyl alkyl chains ($2C_8$) on two different imidazole rings) (**2a–i**) (Scheme 1).

As for anion properties, both mono- and dianions were used. In particular, three monoanions of different sizes, shapes and coordination abilities – bromide, tetrafluoroborate, and bis{(trifluoromethylsulfonyl)}amide ($[NTf_2]^-$) – were used. For the dianions, the presence of two charged head groups on the same spacer could affect the spatial arrangement of cation–anion pairs and, on the whole, the three-dimensional structure of ionic liquids. In order to evaluate the influence due to the different nature of the charged head groups, both sulfonate and carboxylate anions were used. Furthermore, the effect due to the different nature and flexibility of the spacer was also analysed. In this light, both aromatic and aliphatic spacers were considered. In particular, bearing in mind the role played by π–π interactions in determining the structural order, we used aromatic spacers having different degrees of delocalisation. Among carboxylate anions, both 1,4-benzenedicarboxylate $([1,4\text{-bdc}]^{2-})$ and 2,6-naphthalenedicarboxylate $([2,6\text{-ndc}]^{2-})$ anions were used. The pattern of 2,6-substitution on the naphthalene core was also investigated by using the 2,6-naphthalenedisulfonate $([2,6\text{-nds}]^{2-})$ anion. In this case, the effect due to a different isomeric substitution such as the one shown by the 1,5-naphthalenedisulfonate $([1,5\text{-nds}]^{2-})$ anion was also analysed.

In order to evaluate the importance of the rigidity of the spacer between two charged head groups, diimidazolium salts having the 1,4-butanedicarboxylate $([ad]^{2-})$ and 1,6-hexanedicarboxylate $([sub]^{2-})$ anions were also synthesised. The spacers of the above anions were designed to be flexible, but to possess chain lengths similar to those separating the charged head groups in the 1,4-benzenedicarboxylate or 1,5-naphthalenedisulfonate (*cf.* 1,4-butanedicarboxylate) and 2,6-naphthalenedisulfonate or 2,6-naphthalenedicarboxylate (*cf.* 1,6-hexanedicarboxylate) anions.

The thermal stability and melting temperatures, as affected by both cationic and anionic structures, were studied by thermal gravimetric analysis (TGA) and differential scanning calorimetry (DSC).

Results and discussion

Synthesis of dicationic salts

The dicationic bromide was synthesised by using a two-step procedure. In the first step using the 1,3,5-tribromomethylbenzene as the starting material, the neutral precursor 1,3,5-tris-(imidazolemethyl)benzene (**1**)[32] was obtained (Scheme 2). The

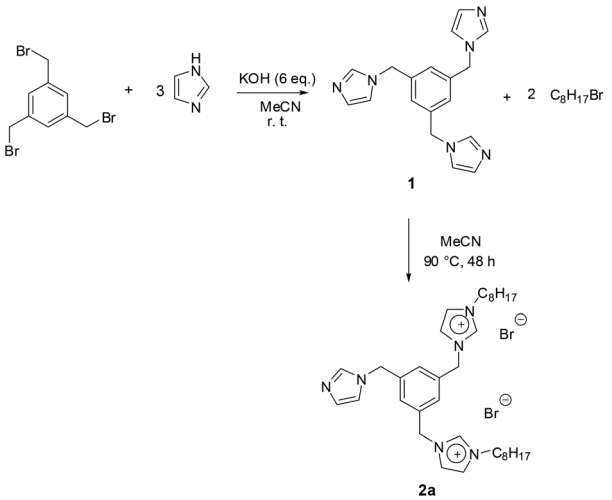

Scheme 2 Schematic representation of the synthesis of diimidazolium bromide.

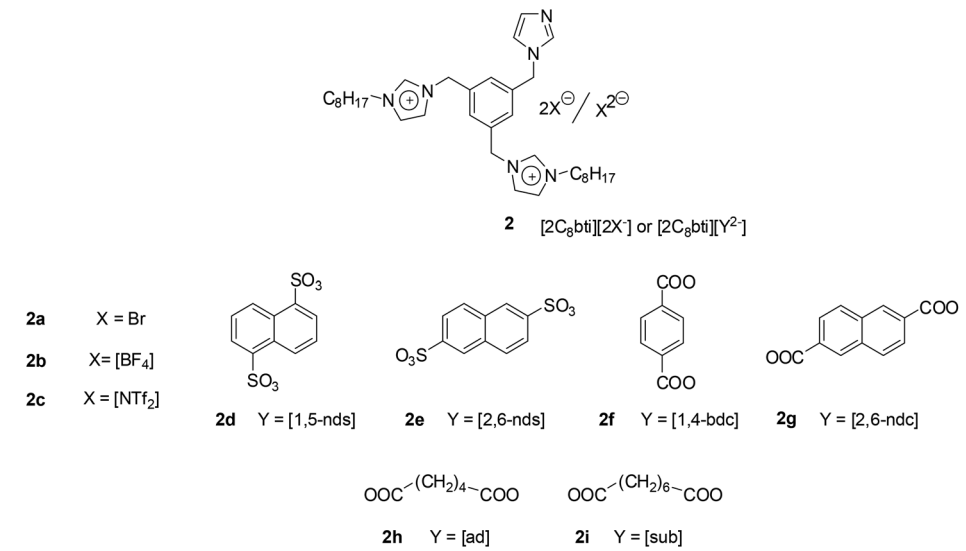

Scheme 1 Structures of dicationic functionalised salts used.

following alkylation of precursor (**1**) in ethanenitrile solution allowed us to obtain the corresponding dibromide salt **2a** (Scheme 2).

In order to carry out the anion exchange, the most widely used metathetic reaction was used to obtain the bistrifylimide derivative.[33] Indeed, most of the salts used in this work showed a very low solubility in conventional organic solvents and we used a previously reported exchange protocol on resin,[34] converting the bromide (**2a**) into the corresponding hydroxide that was subsequently neutralised in the presence of conjugate acids of the anions. According to previous reports, this procedure allowed us to obtain the organic salts with high yields and avoid the use of large volumes of organic solvents.

^{1}H NMR spectroscopic results

First, the behaviour of the diimidazolium salts was studied in dmso-d_6 solution, as a function of the temperature, by using both 1D- and 2D-NMR measurements. Indeed, the ^{1}H NMR spectrum of **2a** at room temperature showed an unexpected signals shape that induced us to suppose the presence of different conformers. Besides, our substrates showed a structural similarity to coelenterand molecules, frequently claimed to possess different conformational isomers.[35] In this light, to verify the presence of different conformational equilibria and to evaluate the effect of the temperature, 1D-NMR spectroscopic measurements were carried out in the range between 300 and 390 K. The temperature range was chosen on the grounds of the freezing point of dmso-d_6 and the highest operational temperature of the NMR spectrometer. In Fig. 1, the ^{1}H NMR spectrum of **2a** in dmso-d_6 solution, recorded at 300 K, is shown. Analysis of the spectrum shows that the benzylic and aromatic protons (5–9.5 ppm) exhibited unexpected signal shapes. Indeed, in both cases the predicted singlets were split into three signals of different intensities. A similar behaviour was detected for all the organic salts utilised in this work. However, in all cases, the spectra were characterised by the presence of "clean" regions (5.0–5.5 ppm and 9.0–10.0 ppm) allowing detection with a good precision of the changes in the shape and chemical shift of the signals.

As previously stated, our organic salts show a structural similarity with flexible coelenterand hosts, which may have different conformations around the central aryl ring.[36–39] For this purpose, Steed and co-workers, studying the behaviour of aminopyridinium hosts,[40] have reported splits of ^{1}H NMR signals at low temperature and ascribed this behaviour to the presence of conformational equilibria. Thus, we hypothesise that, in our case, the observed signals shape could be due to the presence of different conformers in dmso-d_6 solution.

In the range of temperatures chosen, for all the analysed organic salts, we observed both changes in chemical shift values and in the relative area of signals. However, in all cases, the coalescence temperature was outside of the analysed range. In Fig. 2, ^{1}H NMR spectra corresponding to **2d** as a function of temperature are reported (NMR spectra as a

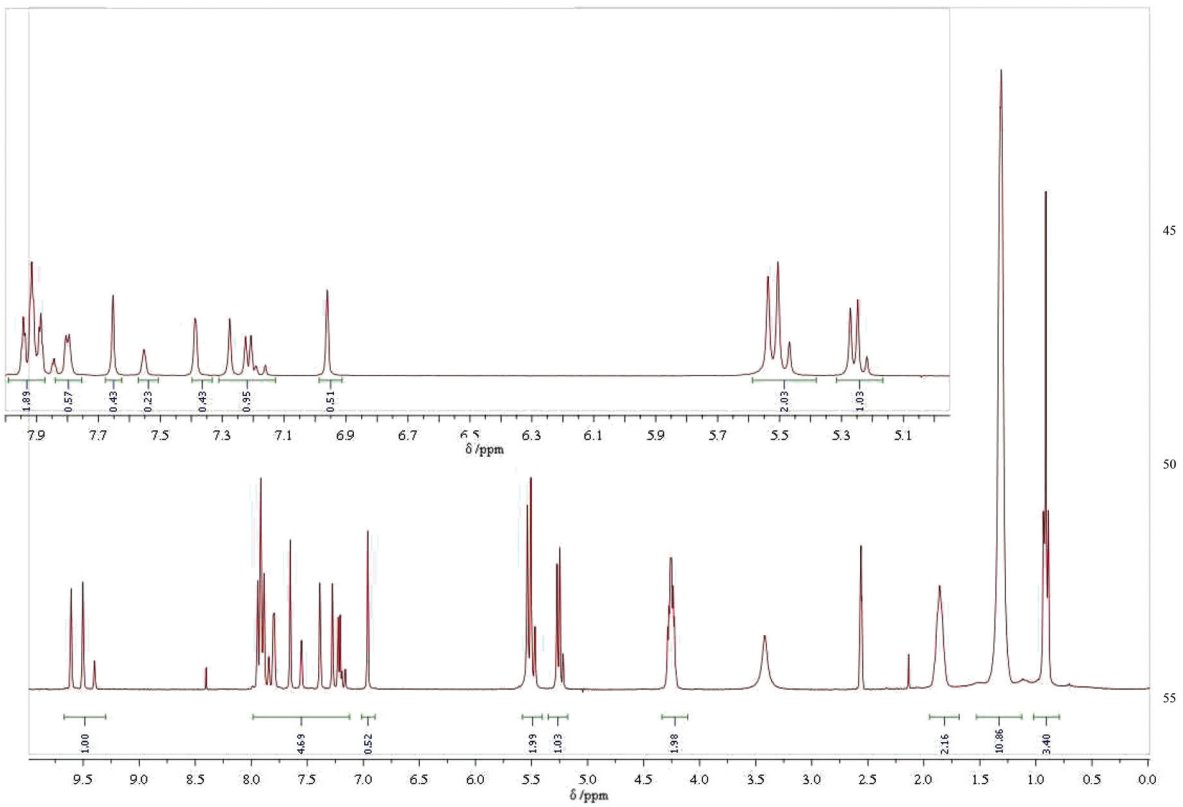

Fig. 1 400 MHz ^{1}H NMR spectrum of **2a** in dmso-d_6 solution (0.038 M) at 300 K (inset: the expanded region 5–8 ppm).

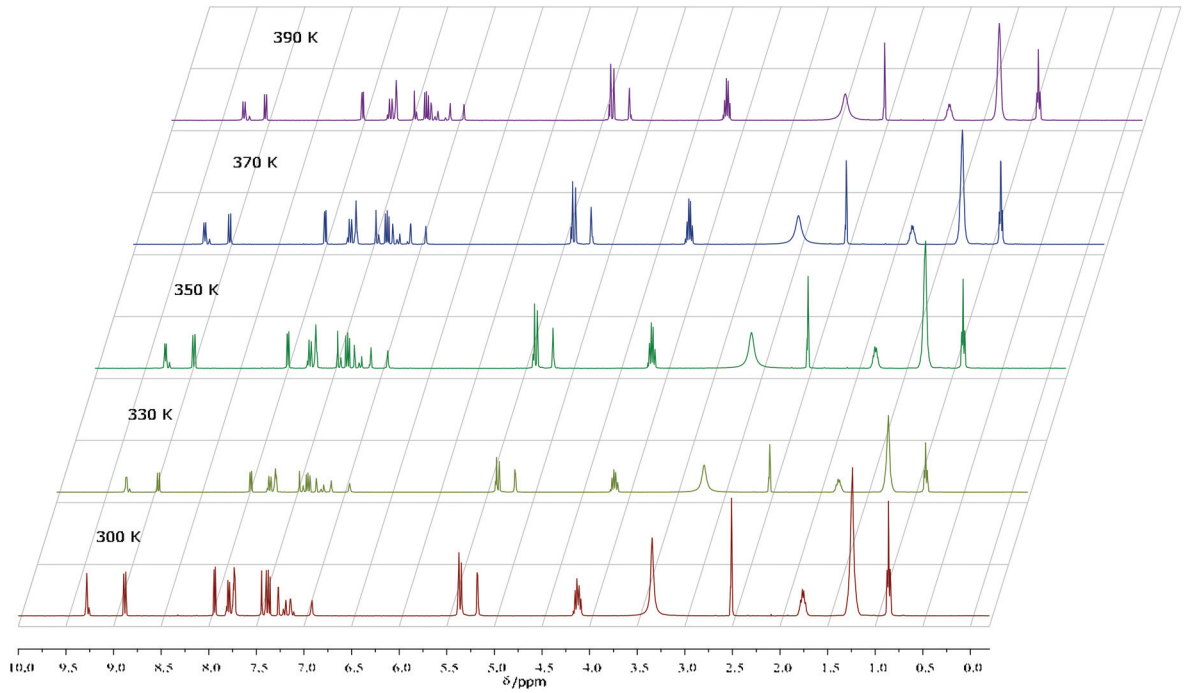

Fig. 2 ^{1}H NMR spectra of **2d** in dmso-d_6 solution (0.038 M) in the range 300–390 K.

function of the temperature, for all organic salts, are reported in Fig. 1 of ESI†).

As the temperature increases, an up-field shift for the H(2) proton of the imidazolium ion (~9.5 ppm) and a down-field shift for the benzylic protons bearing the imidazolium ion (~5.5 ppm) are observed. In general, the extent of the observed shift was more significant for the H(2) of the imidazolium ion than for the benzylic protons ($\Delta\delta_{Hi} \sim +0.05$ and -0.09 ppm for benzylic protons and H(2) of the imidazolium ion, respectively).

Since the analysed protons show very different chemical shifts, our data were plotted as $\Delta\delta_{Hi}(T)$, where $\Delta\delta_{Hi}(T) = \delta_{Hi}(T) - \delta_{Hi}$ (300 K) and examined for the correlation between $\Delta\delta_{Hi}$ and T values. Fig. 3 shows the chemical shift variations for the analysed signals as a function of both the temperature and the different nature of the anion, and the linear regression data are given in Table 1. The equations fitted are given below:

$$\Delta\delta_{H2} = m_1 \times T + m_2 \quad (1)$$

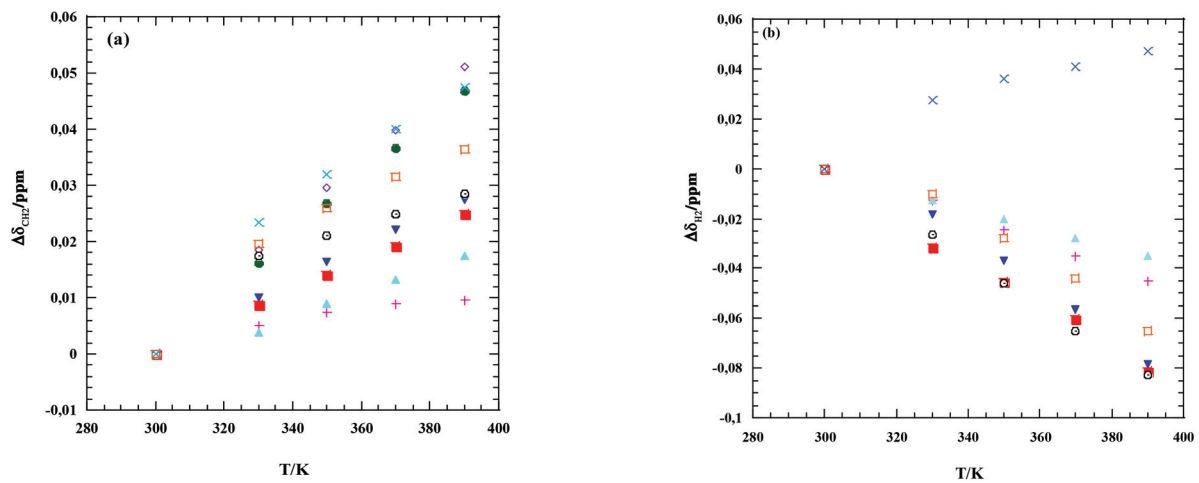

Fig. 3 Plots of $\Delta\delta_{Hi}(T)$ as a function of temperature corresponding to: (a) benzylic protons (~5.5 ppm) and (b) H(2) of the imidazolium ion (~9.5 ppm). Legend: X [2C$_8$bti]Br$_2$ (**2a**); ▼ [2C$_8$bti][BF$_4$]$_2$ (**2b**); □ [2C$_8$bti][NTf$_2$]$_2$ (**2c**); + [2C$_8$bti][1,5-nds] (**2d**); ▲ [2C$_8$bti][2,6-nds] (**2e**); ■ [2C$_8$bti][1,4-bdc]; (**2f**); ○ [2C$_8$bti][2,6-ndc] (**2g**); ◊ [2C$_8$bti][ad] (**2h**); ● [2C$_8$bti][sub] (**2i**).

Table 1 Correlation parameters corresponding to chemical shift variation as a function of temperature for the H(2) of the imidazolium ion and CH_2 attached to imidazolium, according to eqn (1) and (2), *R = correlation coefficient

	Imidazolium ring H(2) protons			CH_2 group attached to imidazolium		
Organic salt	$(m_1 \pm \delta m_1)/10^{-4}$	$m_2 \pm \delta m_2$	R^*	$(m_3 \pm \delta m_3)/10^{-4}$	$m_4 \pm \delta m_4$	R^*
(**2a**)	5.03 ± 0.90	−0.144 ± 0.031	0.955	5.16 ± 0.55	−0.151 ± 0.019	0.983
(**2b**)	−8.77 ± 0.61	0.267 ± 0.021	0.992	3.05 ± 0.89	−0.091 ± 0.003	0.998
(**2c**)	−7.32 ± 0.85	0.225 ± 0.029	0.980	3.94 ± 0.54	−0.115 ± 0.099	0.973
(**2d**)	−5.09 ± 0.17	0.154 ± 0.006	0.998	1.07 ± 0.17	−0.0314 ± 0.006	0.963
(**2e**)	−3.91 ± 0.47	0.117 ± 0.002	0.999	1.99 ± 0.13	−0.060 ± 0.005	0.993
(**2f**)	−8.74 ± 0.40	0.260 ± 0.014	0.996	2.75 ± 0.04	−0.082 ± 0.001	0.999
(**2g**)	−9.28 ± 0.92	0.279 ± 0.003	0.999	3.02 ± 0.56	−0.087 ± 0.002	0.952
(**2h**)	—	—	—	5.62 ± 0.11	−0.167 ± 0.004	0.999
(**2i**)	—	—	—	5.20 ± 0.55	−0.156 ± 0.002	0.999

$$\Delta\delta_{CH2} = m_3 \times T + m_4 \quad (2)$$

It is noteworthy that in the case of 1,6-hexanedicarboxylate and 1,4-butanedicarboxylate ions, we were not able to analyse the experimental trend for the H(2) proton of the imidazolium ion in the whole temperature range. Indeed, in these cases, at 370 K, a significant decrease in the corresponding signal area was detected (Fig. 1h–l of ESI†). Probably, this was a consequence of the acid–base reaction between the carboxylate and the H(2) proton of the imidazolium ion. It is known that aliphatic amines are able to extract the H(2) by the imidazolium ion.[41,42]

This reaction has been frequently reported in the literature and has been widely used to favour carbene complexes.[43–49] However, this reaction seems to be affected by the anion structure. Indeed, it did not occur in the presence of the $[1,4\text{-bdc}]^{2-}$ and $[2,6\text{-ndc}]^{2-}$ anions. Analysis of experimental trends reported in Fig. 3 and correlation parameters reported in Table 1 showed how the temperature effect was different both as a function of the nature of the observed protons as well as the anion nature. Among the observed protons, the highest variation in $\Delta\delta_{Hi}$ was detected for the H(2) proton of the imidazolium ion. Indeed, in this case, slope values ranged from 0.000391 up to 0.000928 ppm K^{-1}, whereas for the benzylic protons these values ranged from 0.000107 up to 0.000562 ppm K^{-1}. Changes in chemical shift values seem to be also affected by the anion nature. As far as benzylic protons are concerned, the highest $\Delta\delta_{Hi}$ were detected for the bromide ion (**2a**) and the anions having aliphatic spacers such as 1,6-hexanedicarboxylate and 1,4-butanedicarboxylate ions (**2h** and **2i**). However, no significant differences were detected between the behaviours of the latter two anions.

A comparison of the data reported in Fig. 3a and 3b shows that in both cases the lowest variations in chemical shift values were detected in the presence of naphthalenedisulfonate anions. Finally, comparable changes in chemical shift values were calculated for $[BF_4]^-$ (**2b**) and $[1,4\text{-bdc}]^{2-}$ (**2f**) anions.

Bearing in mind the possibility of the occurrence of different conformational equilibria, our data seem to indicate a certain relevance of anion properties in determining the conformers distribution in isotropic solution. In particular, significant changes in chemical shift values should be the result of significant changes in the spatial arrangement of the cation structure. In the light of the above considerations, among the tested anions, the naphthalenedisulfonate anions seem to induce the formation of the most tight ion pairs in which only small variations in the cation conformation are allowed.

Recently, some of us have investigated the geometry of the interactions between the 3,3′-dioctyl-1,1′(1,3-phenylenedimethylene)diimidazolium cation and the 1,5-naphtalenedisulfonate anion.[50] In the optimised geometry the anion is embedded in a kind of close cage formed by two aromatic rings of the cation. The sulfonate group of the anion interacts simultaneously through hydrogen bonds with two imidazolium rings belonging to different cations.

A similar geometry could be also effective in our case; this arrangement certainly limits the cation conformational freedom and should be supported by the experimental evidence of cation–anion interactions (see later). The above hypothesis was confirmed by the presence of cross-correlations peaks in 2D NOESY spectra recorded for diimidazolium salts having aromatic dianions. For example, in the case of naphthalenedisulfonate salts (**2d**) and (**2e**) (Fig. 4 of the text and Fig. 2a of ESI†), interactions between benzylic protons in the cation and anion protons (5.34–7.38 ppm for **2d** and 5.14–7.71 ppm for **2e** respectively) were evidenced. On the other hand, for 1,4-benzenedicarboxylate salt (**2f**), in addition to the above interaction (5.41–7.77 ppm), interaction between the H(2) proton of the imidazolium ion and anion protons (10.24–7.77 ppm) was also detected (Fig. 2b of ESI†). In Fig. 4b a schematic representation of possible interactions between the cation and the anion is shown.

Obviously, the variation in chemical shift values depends on the fact that each anion by virtue of its rigidity or flexibility and coordination ability can cause a particular arrangement of cation–anion pairs and as a consequence different conformational equilibria.

DSC measurements

The functionalised dicationic salts were studied using DSC measurements, and the melting point, the enthalpy and the entropy variations relating to the melting process were obtained. Data collected are reported in Table 2, whereas DSC

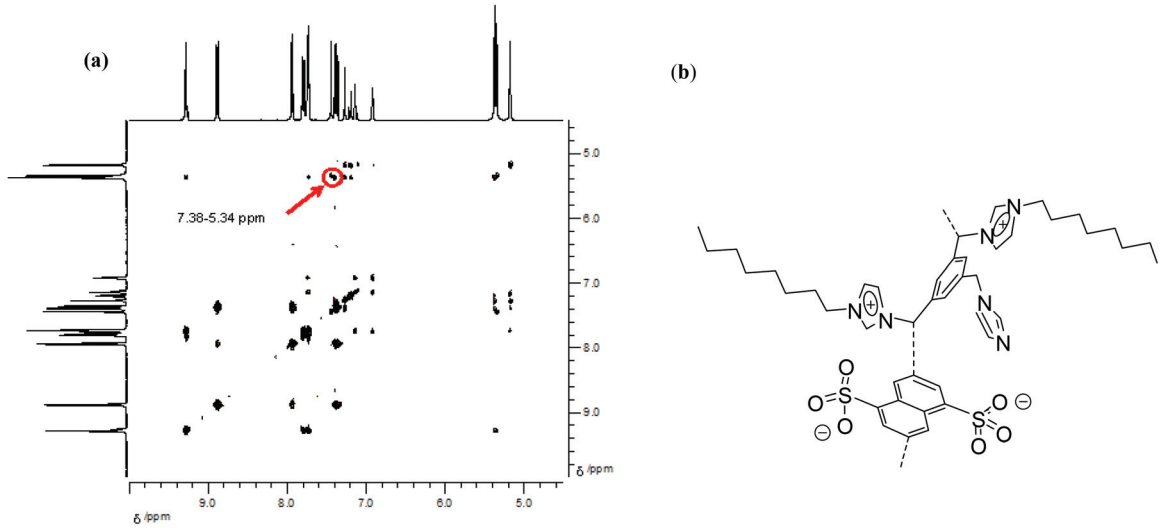

Fig. 4 (a) 2D NOESY spectrum of dicationic functionalised [2C$_8$bti][1,5-nds] (**2d**); (b) schematic representation of the possible interactions leading to the NOESY data.

Table 2 Melting temperatures, thermodynamic parameters determined by DSC measurements and experimental decomposition temperatures (T_{dn}) and percentage of loss in weight (in brackets) determined by TGA measurements relevant to dicationic ionic liquids **2a–i**

Organic salt	T_m/°C	ΔH_m/kJ mol^{-1}	ΔS_m/J mol^{-1} K^{-1}	T_{d1}/°C	T_{d2}/°C	T_{d3}/°C
(**2a**)	53.1	2.4	7.3	235.4 (7.3)	311.8 (56.3)	422.9 (19.2)
(**2b**)	51.1	5.3	16.4	283.3 (18.1)	380.8 (53.7)	461.2 (8.7)
(**2c**)	51.1	4.2	12.9	283.6 (6.5)	436.0 (83.1)	
(**2d**)	55.3	45.9	139.8	289.0 (11.8)	345.5 (56.2)	
(**2e**)	50.4	41.8	129.3	236.2 (7.4)	316.7 (52.7)	485.9 (16.5)
(**2f**)	55.9	5.4	16.2	250.4 (38.9)	340.4 (23.4)	
(**2g**)	—	—	—	245.9 (64.3)		
(**2h**)	51.1	6.2	19.2	228.8 (16)	244.3 (47.1)	351.4 (24.0)
(**2i**)	54.4	8.5	26.0	233.6 (41.3)	373.6 (29.3)	

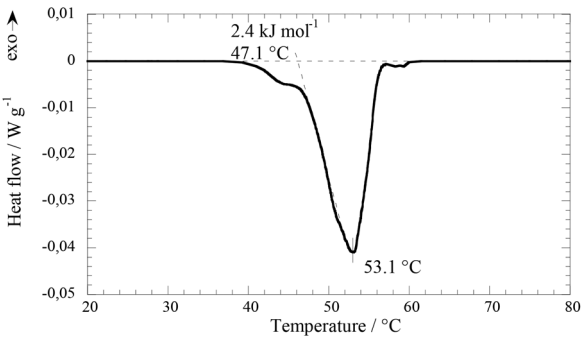

Fig. 5 DSC trace of dicationic functionalised ionic liquid **2a** [2C$_8$bti]Br$_2$.

traces are reported in Fig. 3 of ESI,† and a typical trace is shown in Fig. 5.

We were not able to observe the melting process in the case of **2g** likely due to the small enthalpy variation. For all other systems, the peaks in DSC traces are quite broad, and in some cases shoulders are observed. This result, according to a previous report of Armstrong and co-workers, could be a consequence of the high viscosity of the liquid phases obtained from the melting process.[3] However, as stated above on the basis of NMR measurements and according to previous reports in the literature,[51,52] it could be also complicated by the high flexibility of the cation that can adopt different conformations giving rise to different energies of the crystal lattice and multistep transitions.

Perusal of the data reported in Table 2 allows us to make some observations. Notwithstanding the quite complex cation structure, all the analysed organic salts were able to behave as ionic liquids as accounted for by their melting temperatures. In general, this parameter changes in a narrow range (50.4–57.9 °C), with the lowest value detected for **2e** and the highest for **2f**. Wider ranges have been previously reported for dicationic imidazolium salts having an aliphatic spacer.[3]

Analysis of T_m values evidences how the different nature of the anion induces only small differences. The collected data do not allow us to make a clear distinction between mono- and dianions.

However, taking into account monoanions, the melting temperature decreases on going from **2a** to **2b** and **2c**. This result perfectly agrees with the observation previously reported in the literature about the decrease in melting temperature of ionic liquids induced by the presence of fluorine containing anions.[12,53,54] On the other hand, for dicarboxylate salts the melting temperature increases on going from 1,4-butanedicarboxylate (**2h**) up to 1,4-benzenedicarboxylate (**2f**), outlining a certain influence on the analysed parameter of both the length (**2h–i**) and the nature of the spacer (**2h** and **2f**). In particular,

the presence of an aromatic spacer, the distance between the charged heads being the same, induces a significant increase in melting temperature.

Obviously, the melting temperature should also account for the strength of the cation–anion interactions that give rise to a different packing in the solid state. Then, a higher melting temperature can be confidently ascribed to the presence, also in the solid state, of a tighter ion pair.

Analysis of thermodynamic parameters allows us to have further information about the differences induced by the anion nature. The ΔH_m values increase on going from mono- to dianions and among dianions, they increase on going from carboxylate (**2f–i**) to sulfonate salts (**2d–e**). Among monoanions, ΔH_m increases from bromide (**2a**) to tetrafluoroborate anion (**2b**), according to the increase in anion hydrogen bond acceptor ability. In contrast to the data previously reported by Matsumoto and co-workers,[55] this factor, rather than the symmetry of the anion, seems to be the key factor. Our hypothesis is also supported by the highest change in entropy value detected for the tetrafluoroborate salt (**2b**) accounting for a more extended hydrogen bond network whose melting induces the greatest disturbance.

Furthermore, the highest enthalpy variations associated with the melting process of naphthalenedisulfonate anions seem to remind us of their lowest conformational freedom detected in isotropic solution by means of NMR investigations. Analysis of the data corresponding to dicarboxylate anions shows that the ΔH_m values increase on going from the aromatic 1,4-benzenedicarboxylate anion (**2f**) to the aliphatic ones (**2h–i**), with the 1,6-hexanedicarboxylate salts showing the highest enthalpy variation. The comparison of these values seems to indicate that with an increase in the anion flexibility, the melting process gets enthalpy disfavoured.

As, in the different cases, we found a qualitative correspondence between melting parameters and conformational equilibria, we attempted to correlate ΔH_m with the slope of the linear correlation describing the temperature effect on the chemical shift. For this purpose, in Fig. 5 of the ESI†, a plot of NMR correlation parameters (slope values reported in Table 1) related to benzylic protons as a function of ΔH_m values is reported. Indeed, with the only exception being the data corresponding to **2f**, two distinct linear trends were observed for mono- and dianions, probably indicating that the temperature effect on the cation–anion interactions works to a different extent but in parallel in solution and in the concentrated liquid phase.

TGA measurements

The thermal stability of all the organic salts was investigated by means of TGA experiments. An example of a typical TGA trace is shown in Fig. 6. The TGA traces are reported in Fig. 4 of ESI,† and the decomposition temperatures and the percentage of loss in weight corresponding to the observed degradation steps are reported in Table 2.

With the only exception of **2g**, in all other cases we detect at least two steps in the degradation process.

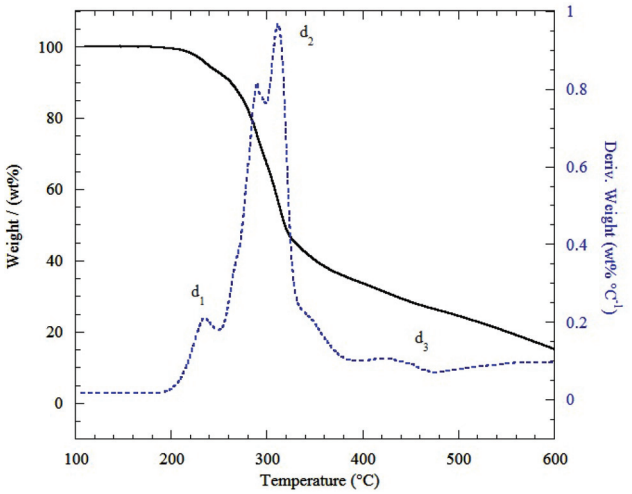

Fig. 6 TGA (black) and DTGA (blue) traces of dicationic functionalised ionic liquid **2a** $[2C_8bti]Br_2$.

In all cases we considered the temperature corresponding to the first degradation step (T_{d1}) as the operational limit for the studied ionic liquids. In this light, the operational limit for the dicationic ionic liquids ranges from 228.8 °C for $[2C_8bti][ad]$ (**2h**) up to 289.0 °C for $[2C_8bti][1,5\text{-nds}]$ (**2d**). However, according to previous reports by Seddon *et al.* the minimum and maximum values should be lowered by 75 and 100 °C respectively.[31,56] In general, our ionic liquids show a lower thermal stability with respect to dicationic pyrrolidinium and imidazolium salts having aliphatic spacers previously reported by Armstrong and co-workers.[3] The very different thermal stability could be a result of the different nature of the spacer used. However, alternatively in our case, it could be also ascribed to the higher substitution degree induced by the presence of the basic functionality in the cation structure that gives rise to the different conformers (see above). Similar results have been previously obtained by analysing the thermal stability of some unsymmetrical dicationic ionic liquids.[3,57,58]

Perusal of the data reported in Table 2 evidences how, differently from the melting process (see above), the decomposition process is significantly affected by the anion nature. Reversible dealkylations of imidazolium salts *via* a nucleophilic attack by the anion could account for the decomposition process. In general, with the only exception of **2e**, in the presence of monoanions, the full degradation process occurs in a larger temperature range with respect to the one detected for dianions. Furthermore, in the series of monoanions, T_{d1} values decrease following the order: $[NTf_2]^- \sim [BF_4]^- > Br^-$. The lowest stability of bromide salt (**2a**) perfectly agrees with the data previously reported about monocationic imidazolium salts and also in this case it could be ascribed to the highest anion nucleophilicity.[59–62]

In going from mono- to dianions, the thermal stability seems to be affected by both the nature of the charged head and the spacer. Indeed, among dianions, the naphthalenedisulfonate salt **2d** shows the highest thermal stability, possibly

Table 3 Temperatures and experimental and calculated weight loss for one CO_2 molecule corresponding to decarboxylation processes of dicationic functionalised salts **2f–i**

Organic salt	Temperature/°C	Weight loss/%	Calc. weight loss/%
$[2C_8bti][1,4\text{-bdc}]$ (**2f**)	143.6	10.5	6.2
$[2C_8bti][2,6\text{-ndc}]$ (**2g**)	92.7	8.7	5.8
$[2C_8bti][ad]$ (**2h**)	99.1	11.6	6.4
$[2C_8bti][sub]$ (**2i**)	92.0	11.8	6.1

due to contributions from π-stacking and unlike the melting process. The different isomeric substitution seems to play a role. Indeed, decomposition temperature decreases in going from **2d** to **2e**. As mentioned before, in all cases we detected multi-step degradation processes.

As far as dicarboxylate salts are concerned, the decomposition temperature increases on going from aliphatic (**2h–i**) to the aromatic spacers (**2f–g**). On this subject, dicarboxylate salts seem to show a further peculiar behaviour. Indeed, their TGA traces were characterised by a significant first loss in weight occurring at temperature values lower than 150 °C that, according to previous reports,[63] should account for a decarboxylation process. In Table 3, temperatures, and experimental and calculated weight loss corresponding to decarboxylation processes of these salts are reported. Perusal of the above values evidences a higher tendency of **2h–i** to decarboxylate as accounted for by a lower difference detected between calculated and experimental percentages of loss in weight. Taking into account the anion aromatic spacers, the increase in the π-surface extension seems to negatively affect the thermal stability, as accounted for by the decrease in decomposition temperatures on going from **2f** to **2g**. On the other hand, a higher flexibility of the spacer induces a higher thermal stability, as testified by the increase in the T_{d1} values on going from 1,4-butanedicarboxylate (**2h**) to 1,6-hexanedicarboxylate (**2i**) salt. Interestingly, the different nature of the charged head seems to be a key factor in determining the thermal stability of the studied ionic liquids, as testified by the comparison of the data relevant to $[2,6\text{-ndc}]^{2-}$ (**2g**) and $[2,6\text{-nds}]^{2-}$ (**2e**) salts.

Conclusions

In the framework of our interest in the synthesis and applications of ionic liquids, we have synthesised a new class of dicationic functionalised ionic liquids – these contain a basic cationic functionality, and either mono- or di-anions with spacer units. The effect of changing the structural parameters was systematically investigated, and (in particular) the VT NMR analysis showed a significant influence of the nature of the anion.

In contrast, DSC results seem to indicate that the anion structure has little effect on the solid–liquid transition, as revealed by the narrow melting temperature range detected, despite the wide range of structurally diverse anions.

The ionic liquids all show multi-step degradation processes. As noted in other TGA studies, the nature of the anion seems to determine not only the degradation temperature, but also the degradation pathway. These materials, however, show a particularly high decomposition temperature, perhaps allowing their use as high temperature reaction media. These data suggest the possibility of having catalytic solvent media that can be used over a wide range of temperatures without the problem of catalyst loss, and with a significant green benefit.

Experimental section

Materials and measurements

1,3,5-Tris(bromomethyl) benzene, 1-bromooctane, imidazole, sodium hydroxide, Amberlite IRA 400 resin, 1,5-naphthalenedisulfonic·$4H_2O$ acid, terephthalic acid, 1,4-butanedicarboxylic acid, 1,6-hexanedicarboxylic acid, 2,6-naphthalenedicarboxylic acid, tetrafluoroboric acid (50% w/w), lithium bis{(trifluoromethyl)sulfonyl}amide, IR 120 PLUS resin, and sodium 2,6-naphthalenedisulfonate were analytical reagents purchased from commercial sources and used as received. Dichloromethane was distilled prior to use.

^{1}H-NMR, $^{13}C\{^1H\}$-NMR, 2D COSY-NMR and 2D NOESY-NMR spectra were recorded using Bruker AV-300 and AV-400 nuclear magnetic resonance spectrometers. Chemical shifts were reported relative to $SiMe_4$. ^{1}H-NMR spectra at variable temperature were recorded using a 400 MHz nuclear magnetic resonance spectrometer at the following temperatures: 300 K, 330 K, 350 K, 370 K, and 390 K.

ESI-MS spectra were recorded using a Waters LCT Premier ES-MS instrument with an Advion Nanomate infusion system.

The temperatures of decomposition, as well as the mass loss, were measured using a TA instrument TGA Q5000 thermogravimetric analyzer, at a heating rate of 5 °C min^{-1} under nitrogen flow. For samples **2f–i** a significant mass loss (*ca.* 10%) observed at *ca.* 100 °C was attributed to the thermally induced decarboxylation processes while samples **2a–e** showed a very small mass loss (<3.0%) in this range likely due to the moisture content. On this basis, samples **2a–e** were kept at 100 °C until the time derivative of weight loss was less than 0.001% min^{-1} to ensure complete solvent evaporation before the heating ramp. The maximum values of the DTGA curves of each thermogram were used as a measure of the decomposition temperature. The mass loss was calculated from the area of the peaks exhibited by the DTG curves.

The melting points were recorded using a TA Instrument DSC (2920 CE). The samples were sealed in TA Tzero aluminium pans with hermetic lids. The instrument was calibrated using indium as the standard. The temperature was ramped from 20 to 100 °C, at 10 °C min^{-1}. The melting temperature and melting enthalpy were determined respectively from the maximum of the signal and from its area. The DSC

chamber was filled with dry nitrogen gas. The melting point of compound **1** was determined with a Kofler.

General procedure for the synthesis of the precursor 1

1,3,5-Tris(imidazolemethyl)benzene (1). The compound was obtained by modifying a procedure reported in the literature.[32]

Imidazole (2.88 g, 0.042 mol) and potassium hydroxide (4.71 g, 0.084 mol) were dissolved in ethanenitrile (375 cm^3) and stirred for 2 h at room temperature. Then 1,3,5-tris(bromomethyl)benzene (5 g, 0.014 mol) was added to the mixture. The reaction mixture was stirred at room temperature for 1.5 h. The mixture was filtered through a Hirsch funnel to remove insoluble salts and the filtrate was concentrated *in vacuo* at 40 °C. The residue was dissolved in $CHCl_3$ (1 l) and was washed with water (6 × 150 cm^3) until the aqueous layer was neutral to pH paper. The organic layer was dried over anhydrous Na_2SO_4 and was concentrated *in vacuo*. Yield 52%. White powder. m.p.: 175.7–179.7 °C. ^{1}H-NMR (300 MHz; dmso-d_6); δ/ppm: 5.25 (s, 6H); 6.95 (s, 3H); 7.16 (dd, J^1_{H-H} = 8.4 Hz, J^2_{H-H} = 0.9 Hz, 6H); 7.75 (s, 3H). ^{13}C-NMR (75 MHz; dmso-d_6); δ/ppm: 49.3; 119.6; 126.3; 128.9; 137.5; 138.9. Elemental Anal. Calcd (%) for $C_{18}H_{18}N_6$ (318.38): C, 67.90; H, 5.70; N, 26.40. Found: C, 67.73; H, 5.65; N, 26.62.

General procedure for the synthesis of the dicationic bromide salt (2a)

To a stirred solution of 1,3,5-tris(imidazolemethyl)-benzene, **1** (2.33 g; 0.00733 mol) in CH_3CN (150 cm^3) was added dropwise a solution of 1-bromooctane (2.5 cm^3; 0.0146 mol or 3.5 cm^3) in CH_3CN (30 cm^3). The reaction mixture was stirred at 90 °C for 48 h under an Ar atmosphere. After concentration *in vacuo* at 40 °C, the residue was washed with diethyl ether (4 × 100 cm^3) under sonication.

1-[1′-Methyleneimidazole]-3,5-di[1′-methylen-3′-octylimidazolium]-benzene dibromide (2a). Yield 92%. A white vitreous solid. m.p.: 53.1 °C. ^{1}H-NMR (300 MHz; dmso-d_6); δ/ppm: 0.92 (t, J_{H-H} = 6.6 Hz, 6H); 1.31 (m, 20H); 1.85 (m, 4H); 4.25 (m, 4H); 5.25 (m, 2H); 5.49 (m, 4H); 6.96 (s, 1H); 7.25 (m, 2H); 7.58 (m, 3H); 7.90 (m, 4H); 9.46 (m, 2H). ^{13}C-NMR (75 MHz; dmso-d_6); δ/ppm: 14.1; 22.2; 25.7; 28.5; 28.7; 29.5; 31.4; 43.9; 49.2; 51.6; 119.7; 122.7; 123.0; 126.8; 127.9; 128.7; 128.8; 129.1; 136.4; 137.5. ESI-MS: m/z (+): 544; m/z (−): 79; 81. Elemental Anal. Calcd (%) for $C_{34}H_{58}Br_2N_6$ (710.67): C, 57.46; H, 8.23; N, 11.83. Found: C, 57.33; H, 8.04; N, 11.98.

General procedure for anionic exchange on basic resin used to obtain dicationic salts (2b, 2d–i)

The compounds were obtained by modifying a procedure reported in the literature.[34]

Compound **2a** was subjected to anion exchange using a basic resin Amberlite IRA-400 with chloride sites. The resin (15.9 g for 0.0037 mol of **2a**) was washed with water. Then it was washed with an aqueous solution of NaOH (804 cm^3, 10% w/v). The excess of the NaOH solution was removed by washing the resin with water until neutrality of pH. Compound **2a** (0.0037 mol) was dissolved in 25 cm^3 of a binary mixture of methanol–water (70/30, v/v). The resin was washed with this binary mixture, so, for a simple elution, the anion exchange of bromide with hydroxide was carried out. A new species of dihydroxide was formed and it reacted with the acid solution (0.0037 mol in 50 cm^3 of methanol–water (70/30, v/v)) of the desired anion. The elution continued until neutrality of pH. After concentration *in vacuo*, the final product was washed with acetone (3 × 30 cm^3) irradiating with an ultrasonic bath.

1[1′-Methyleneimidazole]-3,5-di[1′-methylen-3′-octylimidazolium]-benzene di-tetrafluoroborate (2b). Yield 94%. A yellow waxy solid. m.p.: 51.1 °C. ^{1}H-NMR (300 MHz; dmso-d_6); δ/ppm: 0.92 (t, J_{H-H} = 6.3 Hz, 6H); 1.32 (m, 20H); 1.85 (m, 4H); 4.22 (t, J_{H-H} = 7.2 Hz, 4H); 5.24 (m, 2H); 5.47 (s, 4H); 6.96 (s, 1H); 7.30 (m, 2H); 7.64 (m, 3H); 7.89 (m, 4H); 9.28 (m, 2H). ^{13}C-NMR (75 MHz; dmso-d_6); δ/ppm: 14.1; 22.2; 25.7; 28.5; 28.6; 29.5; 31.3; 44.4; 49.2; 51.6; 119.6; 122.7; 123.0; 126.7; 127.7; 128.7; 128.9; 136.3; 137.5; 139.6. ESI-MS: m/z (+): 544; cation mass = 543.4178; calculated mass = 543.4175; total mass = 717.4282; calculated mass = 717.4234. Elemental Anal. Calcd (%) for $C_{34}H_{52}B_2F_8N_6$ (718.43): C, 56.84; H, 7.30; N, 11.70. Found: C, 56.63; H, 7.18; N, 12.04.

1-[1′-Methyleneimidazole]-3,5-di[1′-methylen-3′-octylimidazolium]-benzene 1,5-naphthalenedisulfonate (2d). Yield 96%. A white solid. m.p.: 55.3 °C. ^{1}H-NMR (300 MHz; dmso-d_6); δ/ppm: 0.91 (t, J_{H-H} = 6.3 Hz, 6H); 1.27 (m, 20H); 1.80 (m, 4H); 4.17 (m, 4H); 5.23 (m, 2H); 5.41 (m, 4H); 6.97 (s, 1H); 7.23 (m, 2H); 7.44 (m, 3H); 7.43 (dd, J^1_{H-H} = 8.1 Hz, J^2_{H-H} = 7.8 Hz, 2H); 7.79 (m, 4H); 7.98 (d, J_{H-H} = 7.2 Hz, 2H); 8.93 (d, J_{H-H} = 8.4 Hz, 2H); 9.33 (m, 2H). ^{13}C-NMR (75 MHz; dmso-d_6); δ/ppm: 14.1; 22.2; 25.7; 28.5; 28.6; 29.5; 31.3; 44.7; 49.1; 51.5; 119.6; 122.6; 122.9; 124.1; 124.2; 127.8; 128.9; 129.2; 129.7; 136.2; 136.3; 136.4; 136.5; 137.5; 144.0. ESI-MS: m/z (+): 544; $m/2z$ (−): 142; total mass = 831.3937; calculated mass = 831.3938. Elemental Anal. Calcd (%) for $C_{44}H_{58}N_6O_6S_2$ (830.15): C, 63.13; H, 7.71; N, 10.04. Found: C, 62.98; H, 7.57; N, 10.17.

1-[1′-Methyleneimidazole]-3,5-di[1′-methylen-3′-octylimidazolium]-benzene 2,6-naphthalenedisulfonate (2e). Naphthalenedisulfonic acid is not commercially available. So, it was obtained from the corresponding sodium salt utilizing the acid resin IR 120 PLUS (15.4 g for 0.0030 mol of salt). The cation exchange was carried out in the same way as the anion exchange. The resin was charged with an aqueous solution of HCl (775 cm^3, 10% v/v). When the naphthalenedisulfonic acid was obtained, the anion exchange was carried out utilising the general procedure described above.

Yield 98%. A white solid. m.p.: 50.4 °C. ^{1}H-NMR (300 MHz; dmso-d_6); δ/ppm: 0.84 (m, 6H); 1.21 (m, 20H); 1.75 (m, 4H); 4.13 (m, 4H); 5.17 (s, 2H); 5.40 (s, 4H); 6.88 (s, 1H); 7.13 (m, 2H); 7.58 (m, 3H); 7.71 (m, 2H); 7.78 (m, 4H); 7.88 (m, 2H); 8.13 (s, 2H); 9.38 (m, 2H). ^{13}C-NMR (75 MHz; dmso-d_6); δ/ppm: 14.3; 22.4; 25.9; 28.7; 28.8; 29.6; 31.5; 44.7; 49.3; 51.8; 119.8; 122.8; 123.3; 124.1; 124.6; 128.0; 128.4; 129.1; 132.3; 136.4; 136.6; 137.7; 139.5; 139.8; 146.3. ESI-MS: $m/2z$ (+): 272; m/z (−): 283. Elemental Anal. Calcd (%) for $C_{44}H_{58}N_6O_6S_2$ (830.15): C, 63.59; H, 7.03; N, 10.11. Found: C, 63.44; H, 7.24; N, 10.01.

1-[1′-Methyleneimidazole]-3,5-di[1′-methylen-3′-octylimidazolium]-benzene 1,4-benzendicarboxylate (2f). Terephthalic acid is insoluble in water and in methanol at room temperature. So, an aqueous suspension was generated and the anion exchange reaction was carried out stirring in suspension.

Yield 95%. A white solid. m.p.: 55.9 °C. ^{1}H-NMR (300 MHz; dmso-d_6); δ/ppm: 0.87 (m, 6H); 1.25 (m, 20H); 1.81 (m, 4H); 4.20 (m, 4H); 5.20 (m, 2H); 5.47 (m, 4H); 6.92 (m, 1H); 7.26 (m, 2H); 7.38 (m, 3H); 7.78 (s, 4H); 7.87 (m, 4H); 10.31 (m, 2H). ^{13}C-NMR (75 MHz; dmso-d_6); δ/ppm: 19.1; 22.4; 27.2; 30.7; 33.5; 33.6; 34.5; 36.3; 54.1; 56.5; 124.6; 127.7; 127.8; 132.9; 133.1; 133.9; 134.5; 137.5; 142.5; 142.6; 146.4; 174.5. ESI-MS: m/z (+): 709; total mass = 709.4454; calculated mass = 709.4441. Elemental Anal. Calcd (%) for $C_{42}H_{56}N_6O_4$ (708.44): C, 71.16; H, 7.96; N, 11.85. Found: C, 71.32; H, 7.88; N, 11.68.

1-[1′-Methyleneimidazole]-3,5-di[1′-methylen-3′-octylimidazolium]-benzene 2,6-naphthalenedicarboxylate (2g). 2,6-Naphthalenedicarboxylic acid is insoluble in water and in methanol at room temperature. So an aqueous suspension was generated and the anion exchange reaction was carried out stirring in suspension.

Yield 98%. A light yellow hygroscopic solid. ^{1}H-NMR (300 MHz; dmso-d_6); δ/ppm: 0.86 (m, 6H); 1.20 (m, 20H); 1.78 (m, 4H); 4.18 (m, 4H); 5.20 (s, 2H); 5.53 (s, 4H); 6.87 (s, 1H); 7.16 (m, 2H); 7.35 (m, 3H); 7.72 (dd, 2H); 7.8 (m, 2H); 7.9 (m, 2H); 8.01 (dd, 2H); 8.34 (s, 2H); 10.23 (m, 2H). ^{13}C-NMR (75 MHz; dmso-d_6); δ/ppm: 14.3; 23.5; 27.1; 29.8; 29.9; 30.9; 32.6; 50.38; 52.8; 52.9; 120.9; 124.1; 128.3; 128.4; 129.4; 129.8; 130.2; 130.9; 134.4; 137.5; 137.8; 138.6; 138.8; 140.4; 140.7; 170.5. ESI-MS: m/z (+): 544; m/z (−): 214. Elemental Anal. Calcd (%) for $C_{46}H_{58}N_6O_4$ (758.45): C, 72.79; H, 7.70; N, 11.07. Found: C, 71.95; H, 7.44; N, 11.86.

1-[1′-Methyleneimidazole]-3,5-di[1′-methylen-3′-octylimidazolium]-benzene 1,4-butanedicarboxylate (2h). Yield 95%. A yellow waxy solid. m.p.: 51.1 °C. ^{1}H-NMR (300 MHz; dmso-d_6); δ/ppm: 0.89 (t, J_{H-H} = 4.8 Hz, 6H); 1.28 (m, 24H); 1.86 (m, 8H); 4.23 (t, J_{H-H} = 6.3 Hz, 4H); 5.23 (m, 2H); 5.50 (m, 4H); 6.94 (m, 1H); 7.30 (m, 2H); 7.60 (m, 3H); 8.06 (m, 4H); 10.50 (m, 2H). ^{13}C-NMR (75 MHz; dmso-d_6); δ/ppm: 14.1; 22.2; 25.8; 27.2; 28.5; 28.6; 29.5; 31.3; 44.7; 48.7; 49.1; 51.4; 119.6; 122.6; 122.7; 122.8; 127.9; 128.9; 129.3; 136.5; 137.6; 137.9; 176.5. ESI-MS: m/z (+): 544; m/z (−): 145; cation mass = 543.4181; calculated mass = 543.4175; anion mass = 145.0484; calculated mass = 145.0501. Elemental Anal. Calcd (%) for $C_{40}H_{60}N_6O_4$ (688.94): C, 69.73; H, 8.78; N, 12.20. Found: C, 69.56; H, 8.58; N, 12.11.

1-[1′-Methyleneimidazole]-3,5-di[1′-methylen-3′-octylimidazolium]-benzene 1,6-hexanedicarboxylate (2i). Yield 94%. A yellow waxy solid. m.p.: 54.4 °C. ^{1}H-NMR (300 MHz; dmso-d_6); δ/ppm: 0.88 (m, 6H); 1.28 (m, 28H); 1.88 (m, 8H); 4.24 (t, J_{H-H} = 7.1 Hz, 4H); 5.23 (m, 2H); 5.50 (m, 4H); 6.93 (s, 1H); 7.33 (m, 2H); 7.63 (m, 3H); 8.02 (m, 4H); 10.50 (m, 2H). ^{13}C-NMR (75 MHz; dmso-d_6); δ/ppm: 14.3; 22.4; 25.9; 26.9; 28.7; 28.8; 29.7; 29.9; 31.5; 48.9; 49.2; 51.6; 116.2; 119.8; 122.9; 127.2; 128.2; 129.1; 136.7; 137.7; 138.0; 139.4; 176.5. ESI-MS: m/z (+): 717; total mass = 717.5082; calculated mass = 717.5067. Elemental Anal. Calcd (%) for $C_{42}H_{64}N_6O_4$ (717.00): C, 70.36; H, 9.00; N, 11.72. Found: C, 69.98; H, 8.76; N, 11.96.

1-[1′-Methyleneimidazole]-3,5-di[1′-methylen-3′ octylimidazolium]-benzene di-bis{(trifluoromethylsulfonyl)}amide (2c). The product was obtained using a procedure reported in the literature.[33]

Yield 54%. A yellow waxy solid. m.p.: 51.1 °C. ^{1}H-NMR (300 MHz; dmso-d_6); δ/ppm: 0.85 (t, J_{H-H} = 6.6 Hz, 6H); 1.25 (m, 20H); 1.79 (m, 4H); 4.15 (t, J_{H-H} = 7.2 Hz, 4H); 5.18 (s, 2H); 5.40 (s, 4H); 6.90 (s, 1H); 7.20 (m, 2H); 7.58 (m, 3H); 7.83 (m, 4H); 9.22 (m, 2H). ^{13}C-NMR (75 MHz; dmso-d_6); δ/ppm: 14.2; 22.4; 25.9; 28.7; 28.8; 29.7; 31.5; 49.4; 51.8; 55.2; 116.2; 117.7; 121.9; 122.8; 123.2; 123.4; 127.9; 128.9; 136.4; 137.6; 139.7. ESI-MS: m/z (+): 1103; total mass = 1105.2787; calculated mass = 1105.2678. Elemental Anal. Calcd (%) for $C_{38}H_{52}F_{12}N_8O_8S_4$ (1105.11): C, 41.30; H, 4.74; N, 10.14. Found: C, 41.07; H, 4.97; N, 9.98.

Acknowledgements

We thank the University of Palermo and MIUR (FIRB 2010RBFR10BF5 V) for financial support. One of the authors (C.R.) thanks QUILL for the hospitality received.

Notes and references

1 M. Freemantle, *An Introduction to Ionic Liquids*, RSC Publications, Cambridge, UK, 2010.
2 P. Wasserscheid and T. Welton, *Ionic Liquids in Synthesis*, Wiley-VCH, Weinheim, Germany, 2nd edn, 2008.
3 J. L. Anderson, R. Ding, A. Ellern and D. W. Armstrong, *J. Am. Chem. Soc.*, 2005, **127**, 593–604.
4 B. L. Bhargava and M. L. Klein, *J. Phys. Chem. B*, 2011, **115**, 10439–10446.
5 J.-C. Chang, W.-Y. Ho, I.-W. Sun, Y.-L. Tung, M.-C. Tsui, T.-Y. Wu and S.-S. Liang, *Tetrahedron*, 2010, **66**, 6150–6155.
6 F. D'Anna, F. Ferrante and R. Noto, *Chem.–Eur. J.*, 2009, **15**, 13059–13068.
7 Y.-S. Ding, M. Zha, J. Zhang and S. S. Wang, *Colloids Surf., A*, 2007, **298**, 201–205.
8 T. Payagala, J. Huang, Z. S. Breitbach, P. S. Sharma and D. W. Armstrong, *Chem. Mater.*, 2007, **19**, 5848–5850.
9 Z. Zeng, B. S. Phillips, J.-C. Xiao and J.-M. Shreeve, *Chem. Mater.*, 2008, **20**, 2719–2726.
10 P. S. Sharma, T. Payagala, E. Wanigasekara, A. B. Wijeratne, J. Huang and D. W. Armstrong, *Chem. Mater.*, 2008, **20**, 4182–4184.
11 M. Trilla, R. Pleixats, T. Parella, C. Blanc, P. Dieudonné, Y. Guari and M. W. C. Man, *Langmuir*, 2008, **24**, 259–265.
12 T. S. Jo, W. L. McCurdy, O. Tanthmanatham, T. K. Kim, H. Han, P. K. Bhowmik, B. Heinrich and B. Donnio, *J. Mol. Struct.*, 2012, **1019**, 174–182.
13 X. Han and D. W. Armstrong, *Org. Lett.*, 2005, **19**, 4205–4208.

14 X. Liua, L. Xiaoa, H. Wua, J. Jing Chen and C. Xia, *Helv. Chim. Acta*, 2009, **92**, 1014–1021.
15 F. D'Anna, S. Marullo, P. Vitale and R. Noto, *Eur. J. Org. Chem.*, 2011, 5681–5689.
16 A. Chinnappan and H. Kim, *Chem. Eng. J.*, 2012, 283–288.
17 T. Liu, L. X. Zhang, L. Q. Sun and A. Q. Luo, *Adv. Mater. Res.*, 2012, **382**, 477–480.
18 C. G. Hanke, A. Johansson, J. B. Harper and R. M. Lynden-Bell, *Chem. Phys. Lett.*, 2003, **374**, 85–90.
19 C. S. Consorti, P. A. Z. Suarez, R. F. De Souza, R. A. Burrow, D. H. Farrar, A. J. Lough, W. Loh, L. H. M. Da Silva and J. Dupont, *J. Phys. Chem. B*, 2005, **109**, 4341–4349.
20 J. Dupont and P. A. Z. Suarez, *Phys. Chem. Chem. Phys.*, 2006, **8**, 2441–2452.
21 A. Triolo, O. Russina, H.-J. Bleif and E. Di Cola, *J. Phys. Chem. B*, 2007, 4641–4644.
22 E. Kowsari and M. R. Ghezelbash, *Mater. Lett.*, 2011, **65**, 3371–3373.
23 D. Fang, J. Yang and C. Ni, *Heteroat. Chem.*, 2011, **22**, 5–10.
24 S. S. Khan and J. Liebscher, *Synthesis*, 2010, 2609–2615.
25 W. Zhu, H. Yang, Y. Yu, L. Hua, H. Li, B. Feng and Z. Hou, *Phys. Chem. Chem. Phys.*, 2011, **13**, 13492–13500.
26 F. D'Anna, S. La Marca, P. Lo Meo and R. Noto, *Chem.–Eur. J.*, 2009, **15**, 7896–7902.
27 F. D'Anna, P. Vitale and R. Noto, *J. Org. Chem.*, 2009, **74**, 6224–6230.
28 F. D'Anna, S. Marullo and R. Noto, *J. Org. Chem.*, 2010, **75**, 767–771.
29 F. D'Anna, S. Marullo, P. Vitale and R. Noto, *Ultrason. Sonochem.*, 2012, **19**, 136–142.
30 F. D'Anna, S. Marullo, P. Vitale and R. Noto, *ChemPhysChem*, 2012, **13**, 1877–1884.
31 S. A. Forsyth, U. Frohlich, P. Goodrich, H. Q. N. Gunaratne, C. Hardacre, A. McKeown and K. R. Seddon, *New J. Chem.*, 2010, **34**, 723–731.
32 H.-K. Liu, W.-Y. Sun, H.-L. Zhu, K.-B. Yu and W.-X. Tang, *Inorg. Chim. Acta*, 1999, **295**, 129–135.
33 L. Cammarata, S. G. Kazarian, P. A. Salter and T. Welton, *Phys. Chem. Chem. Phys.*, 2001, **3**, 5192–5200.
34 I. Dinarès, C. Garcia de Miguel, A. Ibanez, N. Mesquida and E. Alcalde, *Green Chem.*, 2009, **11**, 1507–1510.
35 R. Wang, C.-M. Jin, B. Twamley and J. M. Shreeve, *Inorg. Chem.*, 2006, **45**, 6396–6403.
36 S. Koeller, G. Bernardinelli, B. Bocquet and C. Piguet, *Chem.–Eur. J.*, 2003, **9**, 1062–1074.
37 M. H. Filby and J. W. Steed, *Chem. Rev.*, 2005, **250**, 3200–3218.
38 A. D. Swinburne and J. W. Steed, *CrystEngComm*, 2009, **11**, 433–438.
39 S. A. Diener, A. Santoro, C. A. Kilner, J. J. Loughrey and M. A. Halcrow, *Dalton Trans.*, 2012, **41**, 3731–3739.
40 K. J. Wallace, W. J. Belcher, D. R. Turner, K. F. Syed and J. W. Steed, *J. Am. Chem. Soc.*, 2003, **125**, 9699–9715.
41 F. D'Anna, V. Frenna, R. Noto, V. Pace and D. Spinelli, *J. Org. Chem.*, 2005, **70**, 2828–2831.
42 F. D'Anna, V. Frenna, R. Noto, V. Pace and D. Spinelli, *J. Org. Chem.*, 2006, **71**, 9637–9642.
43 S. A. Forsyth, H. Q. N. Gunaratne, C. Hardacre, A. McKeown, D. W. Rooney and K. R. Seddon, *J. Mol. Catal. A: Chem.*, 2005, **231**, 61–66.
44 H. Yang, X. Han, G. Li and Y. Wang, *Green Chem.*, 2009, **11**, 1184–1193.
45 A. Biffis, L. Gazzola, C. Cristina Tubaro and M. Marino Basato, *ChemSusChem*, 2010, **3**, 834–839.
46 O. Hollóczki, D. Gerhard, K. Massone, L. Szarvas, B. Németh, T. Veszprémi and L. Nyulászi, *New J. Chem.*, 2010, **34**, 3004–3009.
47 M. Gruttadauria, L. F. Liotta, A. M. P. Salvo, F. Giacalone, V. La Parola, C. Aprile and R. Noto, *Adv. Synth. Catal.*, 2011, **353**, 2119–2130.
48 M. G. Gyton, M. L. Cole and J. B. Harper, *Chem. Commun.*, 2011, **47**, 9200–9202.
49 X. Yuan, N. Yan, S. A. Katsyuba, E. E. Zvereva, Y. Kou and P. J. Dyson, *Phys. Chem. Chem. Phys.*, 2012, **14**, 6026–6033.
50 F. D'Anna, P. Vitale, F. Ferrante, S. Marullo and R. Noto, *ChemPlusChem*, 2013, **78**, 331–342.
51 J. D. Holbrey, W. M. Reichert, M. Nieuwenhuyzen, S. Johnston, K. R. Seddon and R. D. Rogers, *Chem. Commun.*, 2003, 1636–1637.
52 J. C. Dearden, *Sci. Total Environ.*, 1991, **109–110**, 59–68.
53 P. S. Sharma, T. Payagala, E. Wanigasekara, A. B. Wijeratne, J. Huang and D. W. Armstrong, *Chem. Mater.*, 2008, **20**, 4182–4184.
54 T. Payagala, Y. Zhang, E. Wanigasekara, K. Huang, Z. S. Breitbach, P. S. Sharma, L. M. Sidisky and D. W. Armstrong, *Anal. Chem.*, 2009, **81**, 160–173.
55 K. Matsumoto and R. Hagiwara, *J. Fluorine Chem.*, 2007, **128**, 317–331.
56 D. R. MacFarlane and K. R. Seddon, *Aust. J. Chem.*, 2007, **60**, 3–5.
57 Z.-B. Zhou, H. Matsumoto and K. Tatsumi, *Chem.–Eur. J.*, 2006, **12**, 2196–2212.
58 Y. Gao, J. M. Slattery and D. W. Bruce, *New J. Chem.*, 2011, **35**, 2910–2918.
59 B. K. Chan, N. Chang and M. R. Grimmett, *Aust. J. Chem.*, 1977, **30**, 2005–2013.
60 Y. N. Hsieh, W. Y. Ho, R. S. Horng, P. C. Huang, C. Y. Hsu, H. H. Huang and C. H. Kuei, *Chromatographia*, 2007, **66**, 607–611.
61 M. C. Kroon, W. Buijs, C. J. Peters and G. J. Witkamp, *Thermochim. Acta*, 2007, **465**, 40–47.
62 Y. N. Hsieh, R. S. Horng, W. Y. Ho, P. C. Huang, C. Y. Hsu, T. J. Whang and C. H. Kuei, *Chromatographia*, 2008, **67**, 413–420.
63 K. Ma, K.-M. Lee, L. Minkova and R. G. Weiss, *J. Org. Chem.*, 2009, **74**, 2088–2098.

